

Phytomass, LAI, and NDVI in northern Alaska: Relationships to summer warmth, soil pH, plant functional types, and extrapolation to the circumpolar Arctic

D. A. Walker,¹ H. E. Epstein,² G. J. Jia,² A. Balsler,¹ C. Copass,¹ E. J. Edwards,¹ W. A. Gould,³ J. Hollingsworth,¹ J. Knudson,¹ H. A. Maier,¹ A. Moody,¹ and M. K. Raynolds¹

Received 19 June 2001; revised 9 November 2001; accepted 13 November 2001; published 31 January 2003.

[1] We examined the effects of summer warmth on leaf area index (LAI), total aboveground phytomass (TAP), and normalized difference vegetation index (NDVI) across the Arctic bioclimate zone in Alaska and extrapolated our results to the circumpolar Arctic. Phytomass, LAI, and NDVI within homogeneous areas of vegetation on acidic and nonacidic soils were regressed against the total summer warmth index (SWI) at 12 climate stations in northern Alaska (SWI = sum of mean monthly temperatures greater than 0°C). SWI varies from 9°C at Barrow to 37°C at Happy Valley. A 5°C increase in the SWI is correlated with about a 120 g m⁻² increase in the aboveground phytomass for zonal vegetation on acidic sites and about 60 g m⁻² on nonacidic sites. Shrubs account for most of the increase on acidic substrates, whereas mosses account for most of the increase on nonacidic soils. LAI is positively correlated with SWI on acidic sites but not on nonacidic sites. The NDVI is positively correlated with SWI on both acidic and nonacidic soils, but the NDVI on nonacidic parent material is consistently lower than the NDVI on acidic substrates. Extrapolation to the whole Arctic using a five-subzone zonation approach to stratify the circumpolar NDVI and phytomass data showed that 60% of the aboveground phytomass is concentrated in the low-shrub tundra (subzone 5), whereas the high Arctic (subzones 1–3) has only 9% of the total. Estimated phytomass densities in subzones 1–5 are 47, 256, 102, 454, and 791 g m⁻², respectively. Climate warming will likely result in increased phytomass, LAI, and NDVI on zonal sites. These changes will be most noticeable in acidic areas with abundant shrub phytomass. *INDEX TERMS*: 0315 Atmospheric Composition and Structure: Biosphere/atmosphere interactions; 1640 Global Change: Remote sensing; 9315 Information Related to Geographic Region: Arctic region; *KEYWORDS*: Arctic, bioclimate zones, biomass, remote sensing, vegetation

Citation: Walker, D. A., et al., Phytomass, LAI, and NDVI in northern Alaska: Relationships to summer warmth, soil pH, plant functional types, and extrapolation to the circumpolar Arctic, *J. Geophys. Res.*, 108(D2), 8169, doi:10.1029/2001JD000986, 2003.

1. Introduction

1.1. Phytomass–Normalized Difference Vegetation Index (NDVI) Relationships Along Climate Gradients

[2] Our principal objective was to understand the variation in vegetation properties along present-day climate gradients and how these relate to satellite-derived vegetation indices in order to better monitor and predict climate-induced changes to

arctic vegetation. Data from the Advanced Very High Resolution Radiometers (AVHRRs) are commonly used to monitor changes in the global patterns and timing of vegetation greenness at regional, continental, and global scales [Goward *et al.*, 1991; Justice *et al.*, 1985; Markon *et al.*, 1995]. Reflectance in the red and near infrared channels of multi-spectral sensors (MSS) is used to calculate and map patterns of the normalized difference vegetation index (NDVI). The NDVI has been used for monitoring and modeling a wide variety of tundra biophysical properties, including aboveground phytomass, gross photosynthesis, leaf area index (LAI), ecosystem respiration rates, and CO₂ and methane fluxes [McMichael *et al.*, 1999; Shippert *et al.*, 1995; Stow *et al.*, 1998; Williams and Rastetter, 1999].

[3] AVHRR data from 1981 to 1991 suggests that the photosynthetic activity of global terrestrial vegetation has increased. The seasonal amplitude of the NDVI increased

¹Institute of Arctic Biology, University of Alaska Fairbanks, Fairbanks, Alaska, USA.

²Department of Environmental Sciences, University of Virginia, Charlottesville, Virginia, USA.

³International Institute of Tropical Forestry, USDA Forest Service, San Juan, Puerto Rico.

7–14% in the boreal region between 45°N and 70°N [Myneni *et al.*, 1997]. These patterns are consistent with changes in the seasonal cycle of atmospheric CO₂ and increases in surface air temperatures. This has led to hypotheses that warmer temperatures have promoted increases in plant growth during the summer [Keeling *et al.*, 1996] and increased respiration in winter [Chapin *et al.*, 1996; Oechel *et al.*, 1997]. Much of the increased photosynthetic activity is thought to be because of a lengthening of the growing season caused by earlier snowmelt [Groisman *et al.*, 1994]. Increased shrub phytomass has been observed in warming experiments [Chapin and Shaver, 1996], and there is evidence from repeated aerial photographs that the density of shrubs is increasing in the warmer areas of arctic Alaska [Sturm *et al.*, 2001]. However, the actual link between greater summer warmth and higher NDVI values in tundra environments has not been established. One objective of this study was to examine trends along spatial climate gradients to see if site specific measurements of LAI, climate, and phytomass are consistent with the global observations of NDVI patterns. Another objective was to extrapolate the results to the circumpolar Arctic using recently developed circumpolar AVHRR-derived NDVI data. We were interested in how NDVI and phytomass patterns varied across the Arctic in relation to bioclimate subzones [Yurtsev, 1994; Elvebakk, 1999; Walker *et al.*, 2002].

1.2. Variation Caused by Parent Material pH

[4] We were also interested in how soil pH affects NDVI and phytomass along the summer temperature gradient. Soil pH affects the availability of essential plant nutrients and a variety of biochemical processes, which in turn influence the species composition, phytomass, and spectral reflectance properties of the vegetation [Walker *et al.*, 1998, 2001]. There is a large difference in the composition of plant communities on soils that are essentially base saturated and those on soils where the exchange complex is saturated with exchangeable acidity. In northern Alaska, most areas of so-called moist acidic tundra (MAT) have organic horizons with pH < 5.0 and mineral B horizons with pH between 5.0 and 5.5. Previous studies have shown that the soil pH break between MAT and moist nonacidic tundra (MNT) is about pH 5.5 for the B horizon [Bockheim *et al.*, 1996]. This break corresponds approximately to that of acidic and nonacidic soil reaction classes for Entisols and Aquepts in the US Soil Taxonomy [Soil Survey Staff, 1996]. To be in nonacidic soil families, the pH of the control section (25–50 cm from the mineral soil surface) should be >5.0 as measured in 0.01 M CaCl₂ in 1:1 soil:water suspension.

[5] MNT was first described at Prudhoe Bay growing on loess deposits along the Sagavanirktok River [Walker and Everett, 1991]. It is also found in association with calcareous bedrock and cryoturbated soils all across northern Alaska [Walker *et al.*, 1987; Walker and Walker, 1996]. In glaciated terrain of the Toolik Lake region, the NDVI patterns were found to be correlated with time since deglaciation and parent material pH [Walker *et al.*, 1995]. Similar relationships between NDVI and soil pH occur at a major soil pH boundary at the northern edge of the Arctic Foothills, Alaska [Walker *et al.*, 1998]. Extensive areas of nonacidic loess and alluvial deposits cover much of the

Arctic Coastal Plain, but there are also extensive acidic sand seas [Carter, 1981]. The Arctic Foothills and Brooks Range are a mix of acidic and nonacidic tundras resulting from complex glacial histories, loess deposition, and different lithologies.

1.3. Variation Caused by Plant Functional Types (PFTs)

[6] Many current approaches to modeling vegetation response to climate change use PFTs to group the multitude of plant species into more manageable groups. These groups are based on a combination of structural and functional attributes that are considered important with respect to ecosystem function [Smith *et al.*, 1996; Steffen *et al.*, 1992; Woodward and Cramer, 1997]. Dynamic global vegetation models (DGVMs) incorporate PFT categories and are considered an improvement over previous equilibrium biogeographical models [Epstein *et al.*, 2000; Kittel *et al.*, 2000]. A key to correctly model the response of vegetation to climate change is to understand how PFTs vary along the natural climate gradient. We were therefore interested in how the phytomass of PFTs varied along the climate gradient and in relationship to soil pH.

2. Methods

2.1. Study Sites: Locations, Climate, and Site Characterization

[7] The study was conducted at 12 locations along two transects, four sites along a western transect from Barrow to Ivtok, and eight sites along an eastern transect from Prudhoe Bay to Toolik Lake (Figure 1a). There were fewer field sites along the western transect because of the general inaccessibility of the region. All the sites along the eastern transect are accessible from the Dalton Highway, whereas those along the western transect are accessible only with helicopter or airplane. The research sites were part of two different projects, and different sampling schemes were used to obtain the ground information. For the western transect, 100 × 100 m grids, with 10 m grid point spacing, were surveyed at each location. For the eastern transect, two 50 m lines were surveyed in vegetation at each location.

[8] The study sites were located on large homogeneous zonal sites in close proximity to climate stations. In the Russian tradition of soil and vegetation science, zonal soils and vegetation develop under the prevailing climate without the confounding influence of extreme snow, soil moisture, disturbance, or unusual soil chemistry [Iysotsky, 1927]. Zonal conditions are generally found on flat areas or gentle slopes with fine-grained soils (silt or clay) with moderate soil moisture. The zonal concept is similar in principle to the climatic climax [Clements, 1928; Walker, 2000]. The sites were chosen to sample the full gradient of MaxNDVI values within the three bioclimate subzones of northern Alaska (Figure 1b) (see section 2.4.1 for explanation of MaxNDVI map). The bioclimate subzones are those used for the Circumpolar Arctic Vegetation Map (Figure 2b) [Walker *et al.*, 2000, 2002]. Where parent material did not permit field sampling under zonal conditions, equivalent locations were selected on parent material that varied from the zonal definition. Examples included the sandy site at Atqasuk, and the sites on carbonate bedrock-derived soils at Ivtok.

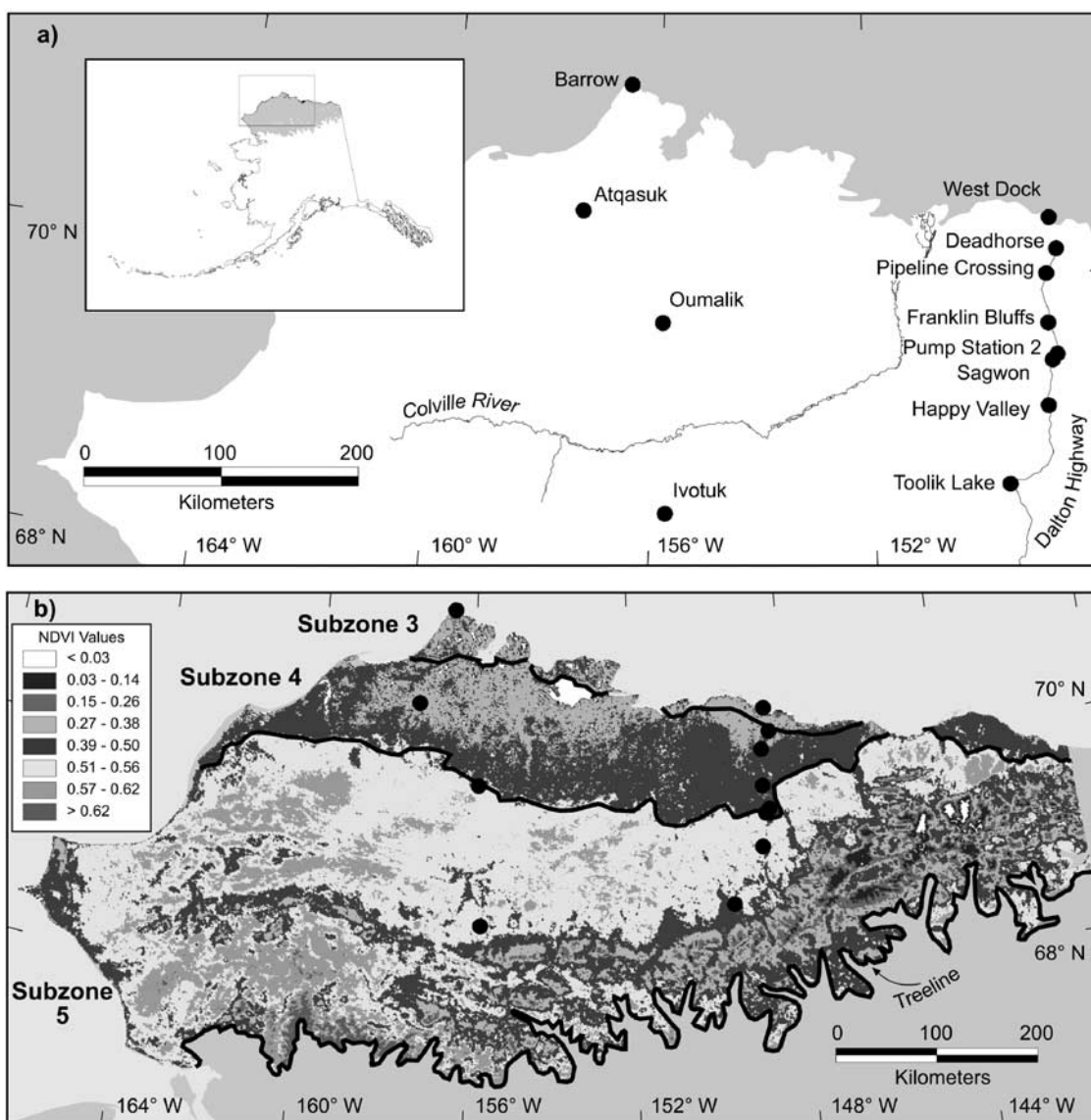


Figure 1. (a) Location of the field study sites on the Arctic Slope, Alaska, along an eastern transect, which follows the Dalton Highway, and a western transect in more remote areas. The inset map shows the tundra area north of treeline in gray. (b) MaxNDVI map of the area north of treeline with the locations of the study areas and the approximate boundaries of the bioclimate subzones. See color version of this figure at back of this issue.

[9] Temperature data for the study sites came from a variety of sources, including the US Weather Services (Barrow, Deadhorse), research sites for the ATLAS study (Atqasuk, Ivotuk), the Long-Term Ecology Research project (Toolik Lake), and other ongoing and previous research projects (Oumalik, Franklin Bluffs, Sagwon, Happy Valley). The summer warmth index (SWI) is the sum of the monthly mean temperatures greater than 0°C . This is the same as the “a” value used to analyze differences in the size of vascular plant floras in relation to summer temperatures [Young, 1971].

[10] The plant community composition at each location was determined using the relevé approach of Braun-Blanquet [Westhoff and van der Maarel, 1978]. The purposes of these samples were to obtain a relatively complete species list for the sites and to use this for

future vegetation classification and gradient analyses. The size of the plots was generally 10×10 m but varied according to the area needed to obtain a complete species list for the site.

[11] Soils were described at each site using USDA protocols [Soil Survey Staff, 1996]. Samples were collected from each soil horizon for physical and chemical analyses. Analyses were performed at the soil laboratory at University of Alaska Fairbanks Palmer Station. We also collected a variety of other information about the site including coordinates, elevation, slope, aspect, landform, parent material, surface geomorphology, site moisture, soil moisture, glacial geology unit, topographic position, exposure to wind, estimated snow duration, site stability, and sign of disturbance. Vegetation, soil, and site data from the western transect were summarized in a data report [Edwards et al., 2000].

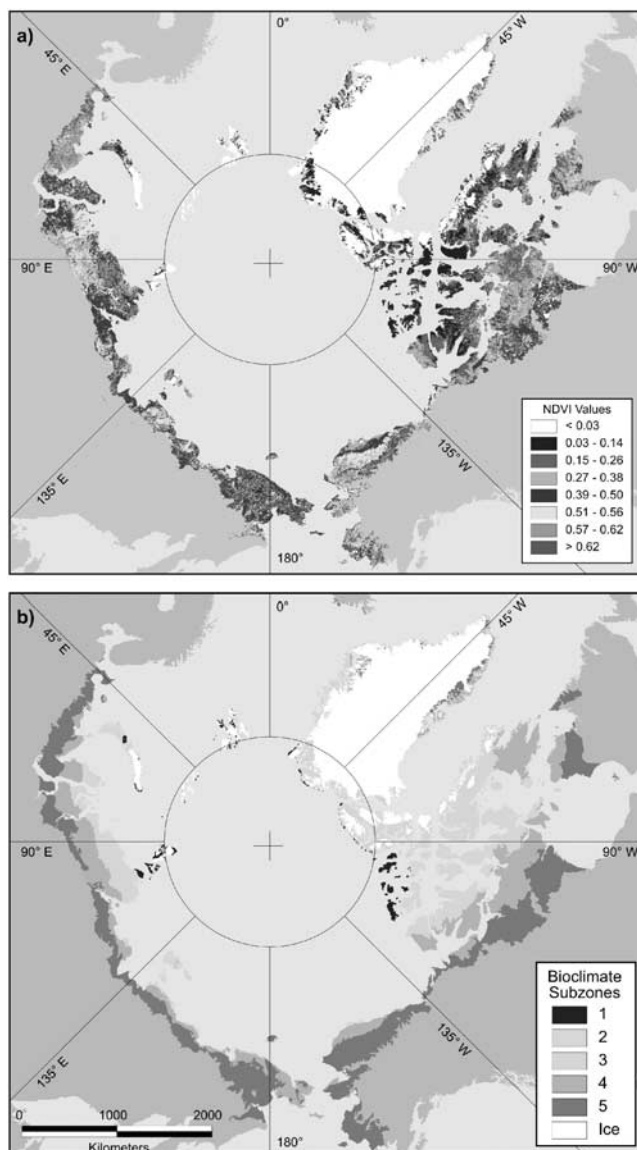


Figure 2. (a) Maximum NDVI of the Circumpolar Arctic. $NDVI = (NIR - R)/(NIR + R)$. NIR is the spectral reflectance in the near-infrared region of the spectrum (0.725–1.1 μm), where light scattering from the canopy dominates. R is the reflectance in the red chlorophyll-absorbing portion of the spectrum (0.58–0.68 μm). The image is derived from the pixels with the highest NDVI among biweekly images from 1993 and 1995 (relatively cloudless and snow-free years). The southern border of the CIR image is clipped to treeline, which was derived from the best available vegetation maps and expert knowledge. (b) Bioclimate subzones of the Arctic Tundra Zone. Subzones 1–5 are equivalent to subzones A–E of Walker *et al.* [2002]. The boundaries of the subzones were modified from the Arctic phytogeographic subzones of Yurtsev [1994] based on more recent information. Subzone 1 is the extreme polar desert subzone with mean July temperatures (MJT) less than 3°C and dominated by bare soil and scattered herbaceous plants, mosses, and lichens and no woody plants nor sedges. Subzone 2 is the prostrate dwarf-shrub subzone with MJT of 3–5°C. Subzone 3 is the hemiprostrate dwarf-shrub (*Cassiope*) subzone with MJT of 5–7°C. Subzone 4 is the erect dwarf-shrub subzone with MJT 7–9°C. Subzone 5 is the low-shrub (40–200 cm tall) subzone with MJT 10–12°C. See color version of this figure at back of this issue.

Data from the eastern transect are available from the first author.

2.2. Phytomass

[12] We determined that a minimum of six random 20 × 50 cm clip-harvest plots were needed to obtain an accurate estimate of the phytomass for each 100 × 100 m grid by

oversampling during the phytomass harvests at our first sample site at Ivotuk. The number of clip harvests per location varied from six to ten. For sites along the western transect, a minimum of six random grid points was selected from the 121 points within the 100 × 100 m grids. Along the eastern transect, three clip harvest were obtained at random points along the two 50 m transects. All vascular

plants were clipped at the top of the moss surface. Green stem bases below the moss surface were also included in the clip harvest. Mosses were carefully trimmed at the base of the green portion. The clip harvests were sorted in the field according to the following PFTs: *shrubs* (plants with woody stems), *graminoids* (plants with grass-like growth forms including grasses, sedges, and rushes), *forbs* (all other nonwoody herbaceous species), *mosses*, and *lichens*. The samples were frozen and returned to the UAF laboratory where they were further sorted into live and dead categories. The shrub category was further divided into foliar, reproductive and stem components. The samples were dried to constant weight at 50°C. Total aboveground phytomass (TAP) values reported here include the erect dead component. We had hoped to use available phytomass data from the Toolik Lake region [Shippert *et al.*, 1995], but decided to exclude these data because differences in the phytomass harvesting methods caused major discrepancies in the phytomass of mosses. No phytomass data were obtained from the Happy Valley site.

2.3. LAI

[13] We used a LICOR LAI-2000 Plant Canopy Analyzer to collect the LAI data. The instrument gives an indication of canopy cover based on differences in diffuse radiation above and below the plant canopy. At each sample point, an above-canopy reading was followed by four below-canopy readings taken above the moss layer. The average of the four readings was retained for the data analysis. A 90° field-of-view shield was used to prevent interference from the observers. All measurements were taken facing away from the Sun. The LAI readings should be taken on cloudy days to prevent problems with reflections in the plant canopy. This was not always possible, so on sunny days an umbrella was used to shade the sensor from direct sunlight while at the same time providing an unobstructed view of the sky. A mean LAI value was calculated for each grid ($N = 33$) and each transect ($N = 50$). We did not make direct comparisons of the optical LAI values with destructive measures of leaf area. A previous study of LAI using the LICOR 2000 instrument in arctic vegetation showed generally good correspondence between LAI, NDVI, and biomass, especially when examined across broad biomass gradients [Shippert *et al.*, 1995].

[14] We collected LAI data from 33 random points within the grids of the western transect. For the eastern transect, we collected LAI at 2 m intervals along two 50 m transects (total of 50 points at each location). Since the sites were generally chosen to be centrally located within large homogeneous zonal landscapes, we assumed that the means of the LAI and biomass were representative of a larger area comparable to an AVHRR pixel. This assumption, however, was not tested.

2.4. NDVI

2.4.1. AVHRR-Derived MaxNDVI

[15] AVHRR-derived NDVI time series data for 1995–1999 were obtained from the U.S. Geological Survey (USGS) Alaska Data Center (ADC) on CD-ROMs. These data were based on 14-day composite periods to match the processing of global data sets. We used the portion of the data between 1 April and 31 October, which consistently brackets the snow-free period in northern Alaska and covers

the greenup-to-senescence phase of the vegetation [Markon, 1999]. Only the portion covering northern Alaska was used for the analysis. The original data were converted into a GRID coverage using ARC/INFO GRID software. Each period throughout the time series was checked for cloud contamination and growing season snow. Cloud and snow contamination were minimized using the Best Index Slope Extraction (BISE) adaptive filter [Ivov, 2000]. The filter is also designed to minimize registration errors that induce short-lived NDVI peaks, which may occur in the compositing process.

[16] We used 1:60,000-scale color-infrared (CIR) aerial photographs (acquisition dates, 1978 and 1982) to delineate 202 areas of homogeneous vegetation on acidic and non-acidic parent material in the vicinity of the climate stations. This was the same data set used by Jia *et al.* [2002] for the analysis of intraseasonal patterns of NDVI in relation to the climate record. Polygons were drawn around these areas with an ink pen on mylar transparent overlays. The aerial photographs and polygons were then digitized and georegistered to the AVHRR imagery using the ARC/INFO software. To register the photographs to the AVHRR image, we used 127 control points from 1:63,360-scale USGS topographic maps. Of the 202 polygons on the aerial photographs, 91 were large enough to locate on the AVHRR image. Although the dates of acquisition for the photographs and the satellite images were different, we assumed that the broad vegetation patterns had not changed, especially within large areas of homogeneous zonal vegetation selected for this study. The mean maximum NDVI (MaxNDVI) for each polygon was calculated from the set of annual maximum NDVI values for all pixels within the polygon. These MaxNDVI values were then used for the correlation analyses with SWI, phytomass, and LAI.

2.4.2. MSS-NDVI

[17] The NDVI value for each pixel was an average spectral reflectance of mosaics of often-very-different surface features within the pixel. The large pixel size (1.1 km) of the AVHRR data caused some problems for the analysis in very heterogeneous landscapes. This was a particular problem on the Arctic Coastal Plain near Barrow and Atkasuk, where thaw lakes and wetland complexes create very complex patterns at subpixel scales. Only 91 of the 202 polygons of homogeneous vegetation that were located on the aerial photographs were large enough to accurately locate on the AVHRR image within similar homogeneous areas. Data from the Landsat MSS has a 70 m pixel size, and it was much easier to find homogeneous areas on the MSS-derived images that correspond to homogeneous areas on the CIR aerial photographs than it was on the AVHRR image. We regressed the NDVI of the MSS pixels within the delineated polygons against the SWI to see if we could improve upon the correlations obtained from the AVHRR 1 km pixels.

[18] The trade-off for smaller pixels in the MSS data is the major reduction in scene size. Northern Alaska is a small portion of an AVHRR image, but required a mosaic of 26 Landsat-MSS scenes. The USGS EROS Data Center in Sioux Falls, SD, produced the mosaic with the Large Area Mosaic Software (LAMS), which is part of the LAS image processing system. The relevant scenes for our analysis were all obtained during the peak phenological

period from mid-July to mid-August and spanned the years from 1976 to 1986. The scenes were radiometrically normalized to a reference scene, meaning that the digital numbers of all the other scenes in the mosaic were modified to correspond with the reference scene in terms of brightness values for comparable image bands. The result was a seamless mosaic that had the appearance of a single image. This image was also used for making the land-cover map of the Arctic Slope [Muller *et al.*, 1999]. All 202 polygons from the CIR photographs were registered to the MSS mosaic, and the mean MSS-NDVI was calculated for each polygon.

2.5. Statistical Analyses

[19] Regression analysis was performed using Microsoft Excel between the following sets of variables: (1) TAP versus SWI, (2) phytomass of PFTs (shrubs, graminoids, moss, and lichens) versus SWI, (3) LAI versus SWI, (4) AVHRR MaxNDVI versus SWI, (5) MSS-NDVI versus SWI, and (6) TAP versus MaxNDVI.

2.6. Circumpolar Extrapolation

[20] An analysis of the trends in MaxNDVI within the five arctic bioclimate subzones was performed using an existing circumpolar MaxNDVI image, which was made for the Circumpolar Arctic Vegetation Mapping (CAVM) project (Figure 2a) [Walker *et al.*, 2002]. The treeline on the image was modified to include the most recent knowledge of members of the CAVM mapping team. We stratified the circumpolar MaxNDVI data (Figure 2a) according to bioclimate subzones (Figure 2b) [Elvebakk *et al.*, 1999]. The subzone boundaries were also modified to reflect the latest knowledge. A regression of TAP as a function of NDVI was developed from data in this study plus information from the literature. Phytomass for low-biomass polar desert sites was obtained from Gilmanov and Oechel [1995]. At the other extreme, phytomass for a tall-shrub site at Council, AK was obtained from C. Copass [unpublished data]. A regression of phytomass versus MaxNDVI was then developed. Phytomass within each subzone was calculated as the sum of the phytomass values in all the pixels in each NDVI class in the given subzone. Analyses were performed for the three subzones on the Arctic Slope, Alaska, and the five subzones in the circumpolar Arctic.

3. Results

3.1. Phytomass

[21] We found that TAP increases with summer temperature on both acidic (MAT) and nonacidic (MNT) parent materials (Figure 3a). The regression lines for MNT and MAT diverge with warmer SWI values. At the coast, the phytomass is similar for both MAT and MNT (about 400 g m⁻²), but at the southern end of the gradient (Sagwon), MNT has about 70% of the phytomass of MAT (932 versus 658 g m⁻²). There is a threefold increase in the SWI, from 9°C to 31°C, and about a 225% increase in phytomass for MAT and about a 50% increase for MNT. The phytomass at Atqasuk is less than that at Barrow (356 versus 451 g m⁻²), despite more than twice the SWI (20.1 versus 9). The cause of this anomaly is thought to be the sandy, leached, nutrient-poor soils at Atqasuk, which lies within a late Pleistocene-age sand sea [Carter, 1981].

[22] We also found major differences in the responses to summer warmth of the dominant PFTs of MNT and MAT. Total aboveground vascular plant phytomass of MAT increases over eightfold, from 82 g m⁻² at Barrow to 719 g m⁻² at Oumalik, whereas MNT vascular plant phytomass shows no significant response to temperature (Figure 3b). All the MNT sites have vascular plant phytomass in the narrow range from 210 to 334 g m⁻² regardless of the amount of summer warmth. Nonvascular plant phytomass (mosses and lichens) show a trend opposite to that of the vascular plants (Figure 3c). We found no significant response of the MAT nonvascular plants to temperature but over a sixfold increase in MNT, from 86 to 575 g m⁻².

[23] When broken down into finer categories, the causes of differences between MAT and MNT phytomass are more apparent. MAT shrubs increase nearly 20-fold from 24 g m⁻² at Barrow to 465 g m⁻² at Oumalik, while MNT shrubs showed essentially no response to temperature (Figure 3d). The regression for MAT shrub phytomass is shown as an exponential function because this was the best fit equation and earlier studies have shown an exponential relationship between summer temperature and shrub height along the same temperature gradient [Walker, 1987]. This curve must level off at somewhat warmer temperatures than encountered along our transects.

[24] We found that MAT moss phytomass is not correlated with SWI, but MNT moss phytomass is strongly correlated, increasing from about 100 g m⁻² near the coast to nearly 500 g m⁻² at the southern end of the gradient (Figure 3e). The phytomass of most PFTs increase across the temperature gradient with the exception of MNT graminoids and MAT lichens (Figure 3f). The steepest responses occur with MAT shrubs and MNT mosses. High lichen phytomass, about 100 g m⁻², occurs on the coastal acidic site at Barrow and the sandy acidic site at Oumalik (Table 1). Forbs and horsetails were abundant at most MNT locations, averaging about 32 g m⁻² compared to about 3 g m⁻² on acidic sites. Over 100 g m⁻² of forbs occur at the Oumalik MNT site, caused mostly by an abundance of arctic lupine (*Lupinus arcticus*).

3.2. LAI

[25] We found that LAI is strongly correlated with SWI on acidic substrates (MAT) ($r^2 = 0.72$, $n = 5$). There is about a 200% increase in MAT LAI across about a threefold increase in summer warmth (Figure 4). We found no correlation between LAI and summer warmth on nonacidic substrates. The 70% increase in phytomass of MNT results in no corresponding increase in measured LAI. Mosses cause most of the increase in MNT phytomass (Figure 3e), and the LAI of the mosses was not measured because the optical sensor of the LICOR LAI-2000 is too large to insert into the moss layer. We consistently rested the sensor on top of the moss layer.

3.3. NDVI

[26] Mean MaxNDVI values show a strong positive correlation with temperature on both acidic and nonacidic substrates (Figure 5a). Nonacidic tundra has generally lower MaxNDVI than acidic tundra. Mean MaxNDVI on acidic substrates varies from 0.36 at Atqasuk to 0.53 at Sagwon, while that on nonacidic substrates varies from

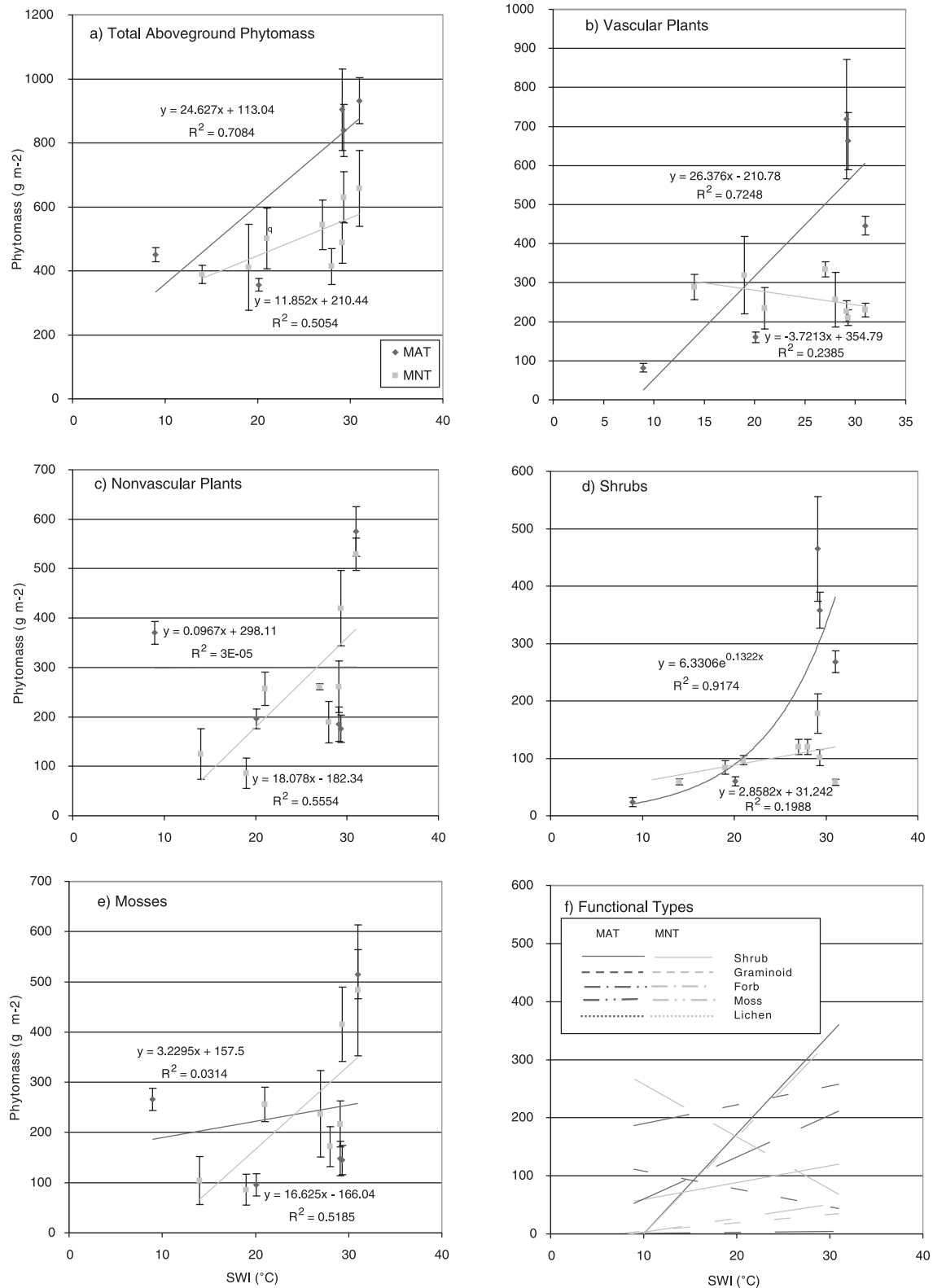


Figure 3. Phytomass (\pm standard error of the mean) along the summer warmth gradient: (a) TAP, (b) vascular plant phytomass, (c) nonvascular plant phytomass, (d) shrubs, (e) mosses, and (f) PFTs. The F statistic for all the regressions are significant at the 0.05 level, except the regressions for acidic nonvascular plants and mosses and nonacidic vascular plants. See color version of this figure at back of this issue.

Table 1. Summary of SWI, NDVI, LAI, and Phytomass for the Study Areas

Site	Veg type	SWI (°C) ^a	MaxNDVI ^b	MSS-NDVI ^c	LAI	Phytomass ± S.E. (g m ⁻²)									
						Total Aboveground	Vascular Plants	Lichens	Mosses	Forbs	Shrubs	Graminoids	Horsetails		
Barrow	MAT	9	0.41	0.32 ± 0.007	0.75 ± 0.02	451 ± 22	82 ± 11	370 ± 23	103 ± 14	266 ± 22	2 ± 1	24 ± 8	55 ± 12	0 ± 0	
Atkasuk	MAT	20.1	0.36	0.16 ± 0.03	1.1 ± 0.02	356 ± 20	160 ± 13	196 ± 20	99 ± 13	96 ± 22	0 ± 0	60 ± 8	101 ± 10	0 ± 0	
Oumalik MAT	MAT	29.1	0.51	0.42 ± 0.04	1.65 ± 0.03	904 ± 127	719 ± 153	185 ± 35	38 ± 13	148 ± 34	2 ± 0	465 ± 91	251 ± 81	0 ± 0	
Ivotuk MAT	MAT	29.3	0.52	0.47 ± 0.04	2.15 ± 0.02	839 ± 81	663 ± 73	176 ± 28	31 ± 8	145 ± 29	3 ± 1	358 ± 31	302 ± 61	0 ± 0	
Sagwon MAT	MAT	31	0.53	0.37 ± 0.02	1.48 ± 0.14	932 ± 72	446 ± 24	575 ± 50	59 ± 15	515 ± 49	9 ± 2	268 ± 19	84 ± 206	0 ± 0	
Toolik Lake MAT	MAT	31.7		0.42 ± 0.01											
Happy Valley	MAT	37.9		0.40 ± 0.02											
West Dock	MNT	14	0.27	0.22 ± 0.08	0.61 ± 0.06	389 ± 29	289 ± 32	125 ± 51	21 ± 12	104 ± 48	25 ± 62	59 ± 5	204 ± 500	0.5 ± 0.4	
Deedhorse	MNT	19	0.39	0.17 ± 0.08	0.89 ± 0.08	411 ± 135	319 ± 99	86 ± 31	6 ± 6	86 ± 31	1 ± 0	84 ± 12	221 ± 38	14.6 ± 5.1	
Pipeline crossing	MNT	21	0.33		0.52 ± 0.05	501 ± 95	234 ± 53	257 ± 34	11 ± 7	256 ± 34	1 ± 0	97 ± 8	122 ± 24	14.0 ± 2.6	
Franklin Bluffs	MNT	27	0.45	0.24 ± 0.07	0.82 ± 0.11	544 ± 77	334 ± 19	261 ± 6	24 ± 14	237 ± 86	54 ± 132	120 ± 13	157 ± 385	2.9 ± 1.7	
Pump Station 2	MNT	28	0.46		0.95 ± 0.11	414 ± 56	257 ± 70	189 ± 42	18 ± 9	172 ± 40	35 ± 86	120 ± 13	97 ± 238	4.7 ± 2.1	
Sagwon MNT	MNT	31	0.48	0.28 ± 0.04	0.49 ± 0.07	658 ± 119	230 ± 17	529 ± 33	46 ± 14	483 ± 130	102 ± 250	58 ± 5	70 ± 171	0.2 ± 0.2	
Oumalik MNT	MNT	29.1	0.37	0.32 ± 0.05	0.61 ± 0.02	488 ± 65	227 ± 27	261 ± 52	45 ± 10	217 ± 46	23 ± 11	178 ± 34	26 ± 3		
Ivotuk MNT	MNT	29.3		0.46 ± 0.05	0.71 ± 0.02	630 ± 80	210 ± 20	420 ± 76	5 ± 3	415 ± 74	15 ± 7	101 ± 14	94 ± 27		
Toolik Lake MNT	MNT	31.7		0.36 ± 0.03											

^aSWI is the sum of the mean monthly temperatures greater than 0°C, derived from station data from the US Weather Service and stations associated with the NSF ATLAS project, courtesy of Larry Hinzman, Doug Kane, Walt Oechel, and Vladimir Romanovsky.

^bMaxNDVI derived from AVHRR biweekly composite data 1993 and 1995, courtesy of USGS Alaska Data Center, Anchorage, AK.

^cMSS-NDVI derived from a mosaic of midsummer Landsat-MSS scenes, courtesy of USGS EROS Data Center, Sioux Falls, SD.

0.27 at West Dock to 0.48 at Sagwon (Table 1). Oumalik and Sagwon have large areas of acidic and nonacidic tundras, so the NDVI of acidic and nonacidic tundra could be determined under the same climate regime at these two sites. At Oumalik, the mean MaxNDVI is 0.51 on acidic soils compared to 0.37 on nonacidic soils, and at Sagwon the MaxNDVI is 0.53 on the acidic sites compared to 0.46 on the nonacidic sites. Atqasuk has a low NDVI compared to the coastal site at Barrow (0.36 compared to 0.41).

[27] MSS-NDVI values show a spatial trend similar to the AVHRR-derived NDVI values, but the correlation with summer warmth is not as strong ($r_{MAT}^2 = 0.26$, $r_{MNT}^2 = 0.40$ for the MSS-NDVI compared to $r_{MAT}^2 = 0.54$, $r_{MNT}^2 = 0.55$ for the AVHRR-derived MaxNDVI) (Figure 5b). The MSS-derived NDVI values are somewhat lower than the AVHRR values and trend toward convergence at the higher SWI values. The high MNT MSS-NDVI at Ivotuk (mean = 0.46) is probably caused by the nonoccurrence of MNT on flat sites at Ivotuk. All the MNT sites at Ivotuk of sufficient size to be discerned on the satellite image are on moderate south-facing slopes, and these sites generally have higher shrub cover than flat sites.

3.4. Circumpolar Extrapolation

[28] Our estimate of the size of the study area in northern Alaska is about 492,500 km² (Table 2), or about 6.9% of the total area within the Arctic. Of this area, subzone 3 covers about 1.5%, subzone 4, 15.6%, and subzone 5, 82.9%. subzone 3 has only about 0.4% of the total phytomass in northern Alaska, and subzone 5 had over 90% of the total. Using the regression of phytomass versus NDVI (Figure 6), we calculated the mean phytomass densities within subzones 3–5 on the Arctic Slope to be 290, 589, and 1096 g m⁻² respectively. These values were somewhat higher than the comparable values for the circumpolar subzones (Table 3).

[29] Our estimate of the area of the circumpolar Arctic is 7,114,924 km² (Table 3). Of this area, subzone 1 covers 1.6%; subzone 2, 5.5%; subzone 3, 15.4%; subzone 4, 22.8%; and subzone 5, 26.2% (Figure 7). Another 18.6% is ice covered. Most of the phytomass (60.7%) is in subzone 5. The estimated mean phytomass densities for the circumpolar subzones are subzone 1, 47 g m⁻²; subzone 2, 256 g m⁻²; subzone 3, 102 g m⁻²; subzone 4, 454 g m⁻²; and subzone 5, 791 g m⁻².

4. Discussion

4.1. Phytomass

[30] The phytomass values reported here for the Arctic Slope fall generally within the values in the literature for zonal Typical Tundra (subzone 4) and Southern Tundra (subzone 5) [Gilmanov and Oechel, 1995]. There is, however, large variation in values reported from the literature because of heterogeneity in collection sites, inconsistent methods between investigators for collecting phytomass data, and difficulty of placing the sites within the proper subzone. It is difficult to relate such data to summer temperature trends and to NDVI values. The phytomass information collected for this study has the advantage of

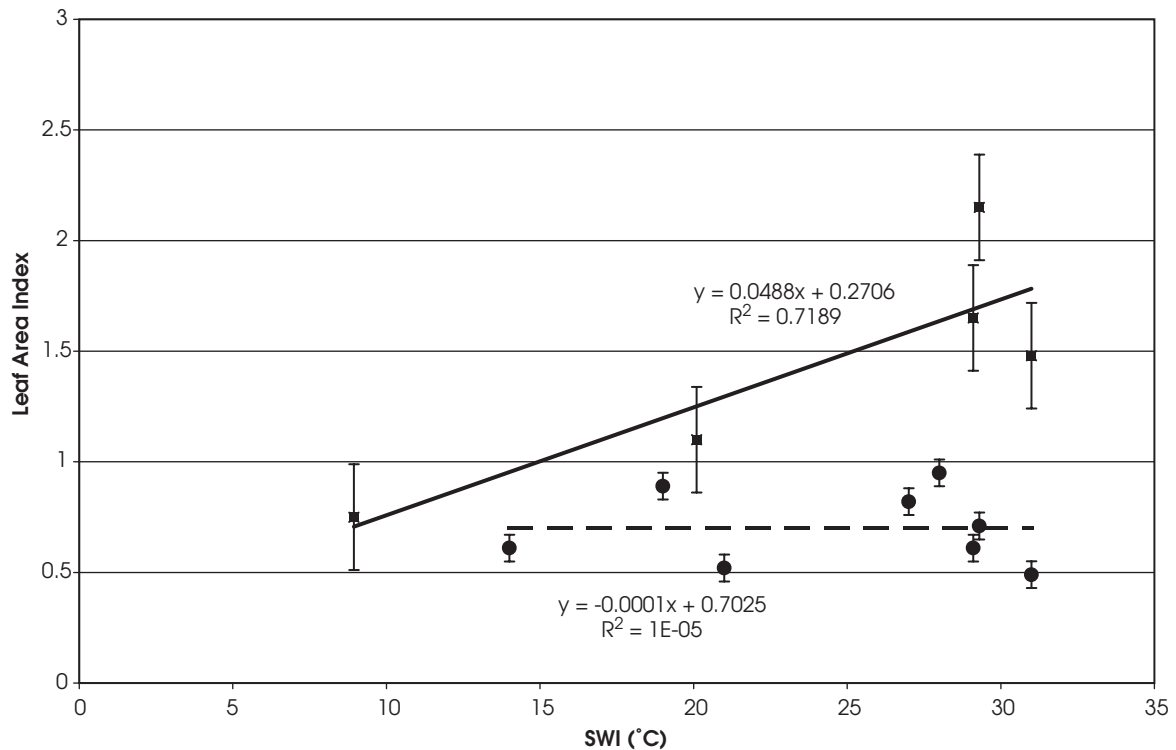


Figure 4. LAI versus SWI.

being collected in a consistent manner from zonal sites specifically for the purpose of correlating the data with local climate information and NDVI information from the same and locally similar sites.

[31] The regression of TAP versus NDVI (Figure 3a) provides a basis for predicting the possible effects of summer warming in much of the Low Arctic. It is a reasonable assumption that temporal changes to NDVI resulting from climate change might replicate the differences that occur along spatial climate gradients because increased warming is likely to cause increased shrub growth [Chapin *et al.*, 1996; Sturm *et al.*, 2001]. The amount of shrubs is strongly correlated with NDVI and summer warmth, particularly in acidic tundra. A 5°C increase in the SWI is approximately equivalent to a 1–2°C increase in the mean July temperature. A 5°C increase in the SWI results in about a 123 g m⁻² increase in the aboveground phytomass for zonal vegetation on acidic sites, and about 60 g m⁻² on nonacidic sites. A similar change could conceivably occur with a 1–2°C change in the mean July temperature caused by global warming.

[32] MAT and MNT show nearly the opposite trend for phytomass of vascular plants and nonvascular plants (Figures 3b and 3c). Shrubs cause most of the increase in MAT phytomass (Figure 3d), whereas mosses cause most of the increase in MNT phytomass (Figure 3e). The reasons for the discrepancy in the shrub response are major differences in the species composition of acidic and nonacidic tundras. The dominant shrubs in MAT are *Salix pulchra* and *Betula nana*. These shrubs exhibit large changes in growth form with increased temperature. For example, in subzone 3, *S. pulchra* has a creeping prostrate

form, rarely exceeding a height of 5 cm. In subzone 3, *S. pulchra* plays a minor role in the overall plant canopy. In subzone 5, *S. pulchra* and *B. nana* are much taller (greater than 40 cm) and play a dominant role in the plant canopy. The shrubs in MNT have a less plastic response to temperature. In MNT, *Dryas integrifolia*, *Salix reticulata*, and *Salix arctica* are the dominant shrubs, and all are very short or prostrate, and show little change in height in response to temperature. The dominant MNT erect shrubs are *Salix richardsonii* and *S. glauca*, but these are usually scattered and do not form a major component of the MNT plant canopies, even at the southern end of the temperature gradient.

[33] The large response of MNT mosses to increased summer warmth (Figure 3e) was an unexpected result. Previous studies have noted that mosses greatly affect the thermal, hydrologic, and nutrient properties of the soils, and are one of the main factors that control the transition of zonal vegetation from MNT to MAT near the southern boundary of subzone 4 [Walker *et al.*, 1998]. More extensive phytomass data from other transects across the Low Arctic would help determine if the pattern of greater MNT moss biomass with warmer temperatures also occurs elsewhere.

[34] We also found major differences in other PFTs on acidic and nonacidic soils (Figure 3f). For example, forbs and horsetails are much more abundant on nonacidic soils. This is consistent with previous observations [Walker *et al.*, 1998; Gough *et al.*, 2000]. High amounts of *Cladina* lichens occur in association with sandy acidic substrates, such as those at Atqasuk, and account for the light spectral signatures of vegetation observed on upland sites here and elsewhere in the sand sea west of the Colville River. The

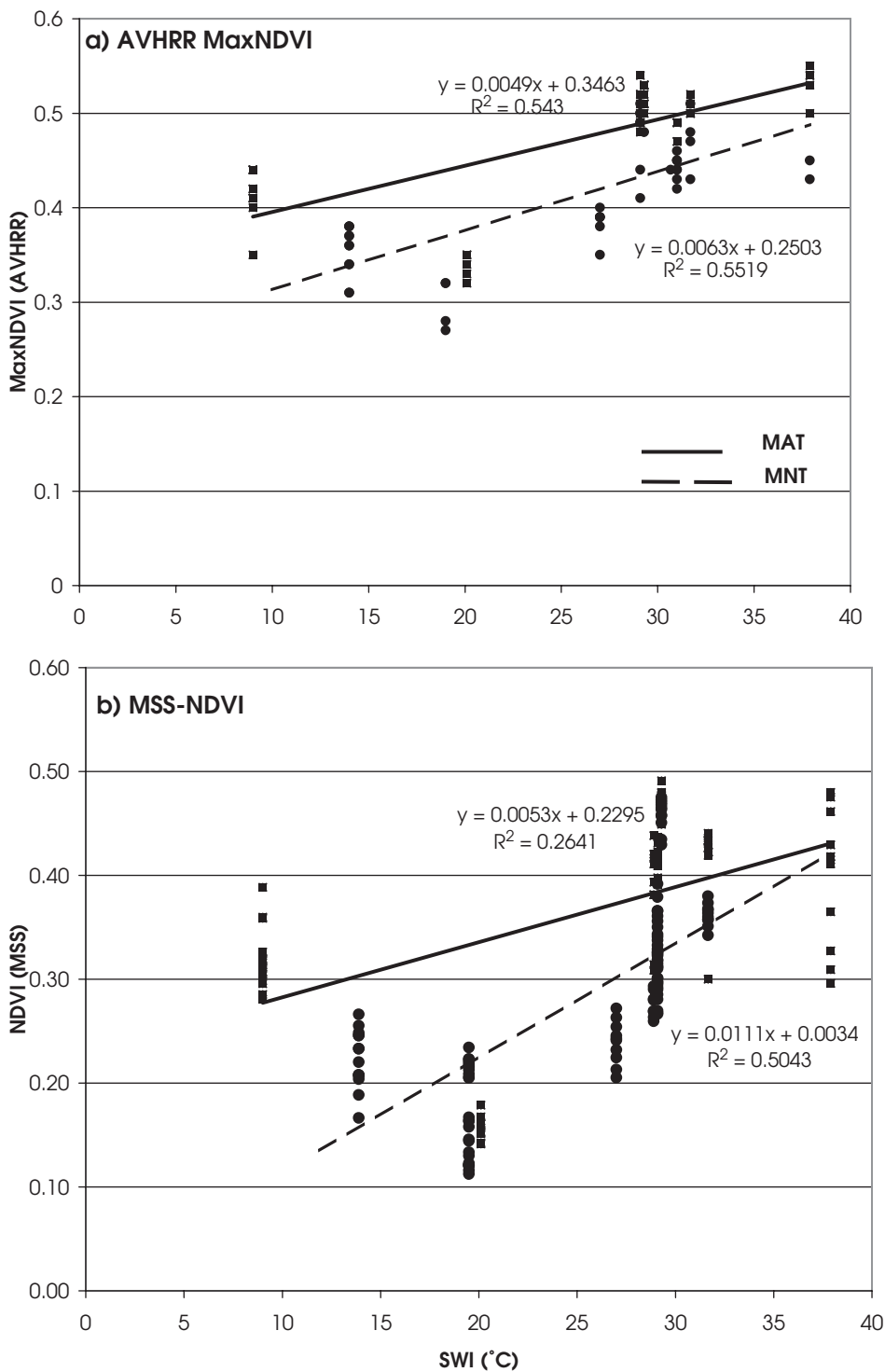


Figure 5. NDVI versus SWI. (a) MaxNDVI derived from the AVHRR biweekly composites. (b) MSS-NDVI derived from an Arctic Slope mosaic of 26 Landsat-MSS scenes provided courtesy of the USGS Alaska Data Center.

large amount of lichens at Barrow may be caused by the humid maritime conditions at this site.

4.2. LAI

[35] The correlation between SWI and measured LAI is relatively strong for MAT ($r^2 = 0.72$), but there was no correlation for MNT (Figure 4). At least along the transect

of this study, mosses cause most of the increase in MNT phytomass, and the LAI of the moss canopy could not be measured by the method of this study (see section 3.2).

4.3. NDVI

[36] Previous studies of NDVI–biomass relationships within single arctic vegetation types have concluded that

Table 2. Area and TAP in Gigagrams (10^{12} g) for the Three Arctic Subzones in Northern, Alaska (see Figure 1 for Area of Analysis)

NDVI class	Phytomass, g m^{-2}	Subzone 3		Subzone 4		Subzone 5		Ice		Total for N. Alaska	
		Area, km^2	TAP, Gg								
0.00	0	1333	0.00	5782	0.0	10,362	0.0	168	0.0	17,645	0.0
0.08	44	29	0.00	72	0.0	3734	0.1	165	0.0	4000	0.1
0.21	112	314	0.03	409	0.0	9319	1.0	107	0.0	10,149	1.1
0.33	256	3802	1.00	15,891	4.2	23,503	6.2	35	0.0	43,231	11.4
0.45	626	1637	1.02	42,741	26.7	99,723	62.4	10	0.0	144,111	90.2
0.54	1194	8	0.01	11,679	13.9	181,801	217.0	0	0.0	193,488	231.0
0.60	1835	0	0.00	139	0.2	61,575	113.0	0	0.0	61,714	113.2
0.65	2626	0	0.00	7	0.0	18,199	47.7	0	0.0	18,206	47.8
Total for northern Alaska	7123	2.07	76,720	45.25	408,216	447.7	485	0.0	492,544	495.1	
% of northern Alaska	1.4	0.4	15.5	9.1	82.8	90.4	0.1	0.0	100.0	100.0	
Phytomass density (g m^{-2})		290		589		1096				1006	

Column 1 contains the midpoints of the NDVI classes in Figure 5a. Column 2 is the phytomass at these midpoints calculated from the regression equation in Figure 6.

biomass is only one of several factors influencing the NDVI, and that these other factors often obfuscate the relationship between NDVI and biomass [Hope *et al.*, 1993]. However, when studied over broad regions and across major changes in vegetation biomass, as in this study, there is a clear relationship between temperature, biomass, and NDVI on mesic zonal sites. Higher NDVI values occur in association with warmer temperatures and larger amounts of aboveground phytomass. This is encouraging for application of NDVI for monitoring trends in global NDVI patterns related to future temperature change. It is also encouraging that the regression lines for the MSS-

and AVHRR-derived NDVI show generally the same trends. However, it is surprising that using the MSS-sized pixels did not improve the correlation between temperature and NDVI over that of the 1 km pixels of the AVHRR pixels. The correlation between the MSS and AVHRR-derived NDVI values is rather low ($r^2 = 0.51$, $n = 10$). This suggests that the radiometric normalization that was done to create the MSS spectral data produced a product that is not as useful as the AVHRR product for large-area comparisons of NDVI. The MSS product is probably more useful for examining NDVI within relatively small regions where the size of homogeneous areas of zonal vegetation is generally

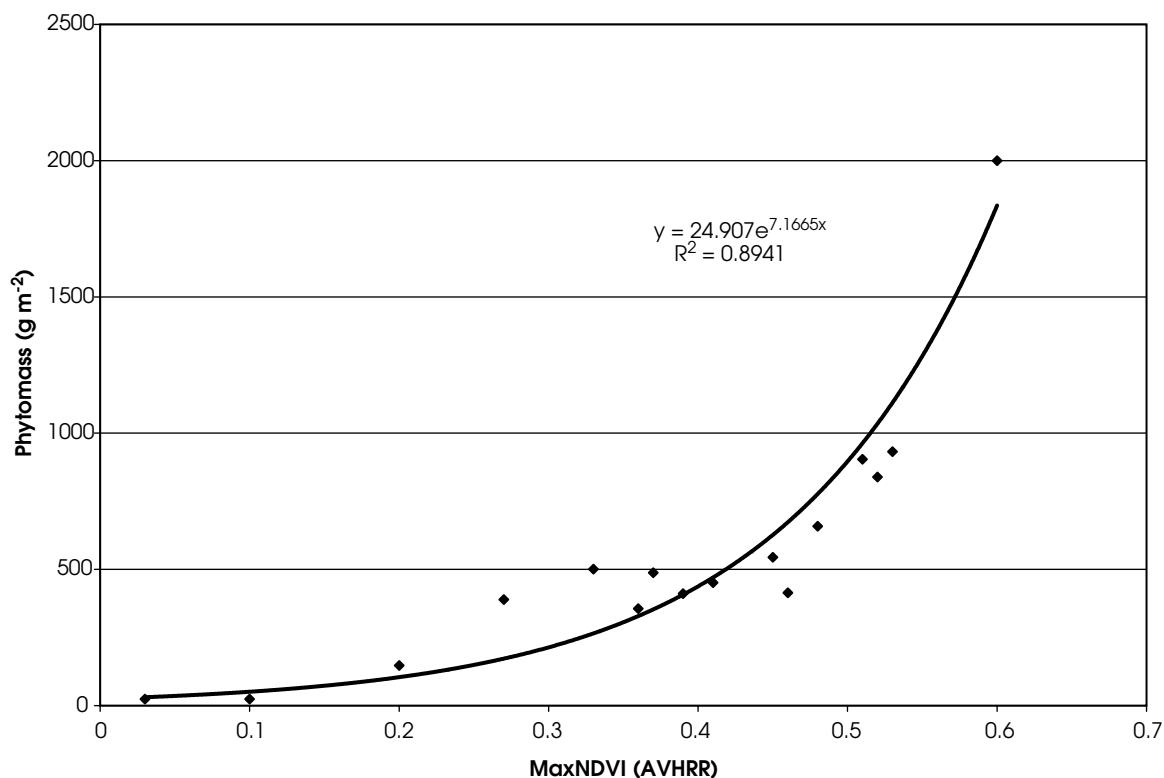


Figure 6. MaxNDVI versus total phytomass. The regression is based on the data from this study plus other information from the literature at the end points of the Arctic climate gradient. The High Arctic sites of Devon Island, Eureka, and Resolute were used for the cold end of the gradient [Gilmanov, 1997], and a shrub tundra site at Council, AK (Copass, unpublished data) was used for the warm end of the gradient.

Table 3. Area and TAP in Gigagrams (10^{12} g) for the Five Arctic Subzones and Total Arctic

NDVI class	Phytomass, $g\ m^{-2}$	Subzone 1		Subzone 2		Subzone 3		Subzone 4		Subzone 5		Ice		Total for Arctic Zone	
		Area, km^2	TAP, Gg	Area, km^2	TAP, Gg	Area, km^2	TAP, Gg	Area, km^2	TAP, Gg	Area, km^2	TAP, Gg	Area, km^2	TAP, Gg	Area, km^2	TAP, Gg
0	0	41,862	0	110,615	0.000	259,798	0.000	122,108	0.000	131,140	0.000	1,837,097	0	2,502,620	0.000
0.08	44	48,614	2.148	174,553	7.713	379,332	16.762	94,923	4.195	34,444	1.522	29,372	0	761,238	32.340
0.21	112	15,717	1.763	57,913	6.497	399,922	44.864	298,726	33.511	86,739	9.730	5383	0	864,400	96.365
0.33	265	2283	0.605	44,168	11.709	166,968	44.263	331,793	87.957	320,096	84.856	1532	0	866,840	229.390
0.45	626	144	0.090	20,439	12.804	101,529	63.603	360,332	225.731	716,882	449.093	422	0	1,199,748	751.321
0.54	1194	6	0.007	5489	6.554	42,600	50.864	170,754	203.879	444,166	530.331	25	0	663,040	791.636
0.6	1835	1	0.002	395	0.725	2183	4.007	42,127	77.322	174,605	320.480	11	0	219,322	402.536
0.65	2626	23	0.060	86	0.226	55	0.144	1679	4.410	51,712	135.817	38	0	53,593	140.657
Total for Arctic Zone	108,650	5	413.658	46	1,352.387	224	1,422.442	637	1,959.784	1,532	1,873.880	0	7,130,801	100,000	2444
% of Arctic Zone	1.52	0.191	5.80	1.891	18.97	9.185	19.95	26.061	27.48	62.671	26.28	0.000	100.00	100,000	343
Phytomass density, $g\ m^{-2}$		43		112		166		448		782		0		343	

much less than a square kilometer, such as on the Arctic Coastal Plain.

[37] The spatial changes in NDVI related to temperature are fairly subtle. An increase of about $5^{\circ}C$ in the SWI amounts to an AVHRR MaxNDVI increase of about 0.03 in acidic tundra and 0.05 in nonacidic tundra. Future changes caused by climate warming may be difficult to detect considering the heterogeneity of arctic landscapes. Small increases in biomass may be difficult to detect in areas where there is a large component of bare rock, such as in shield areas, or areas with a large component of lakes, such as in coastal plains and large deltas. Rock and clear water have NDVI values near zero. A good strategy for monitoring change in NDVI in the Arctic would be to select large areas with relatively homogeneous zonal vegetation, such as tussock tundra that broadly occurs in the Arctic Foothills in northern Alaska [Jia *et al.*, 2002].

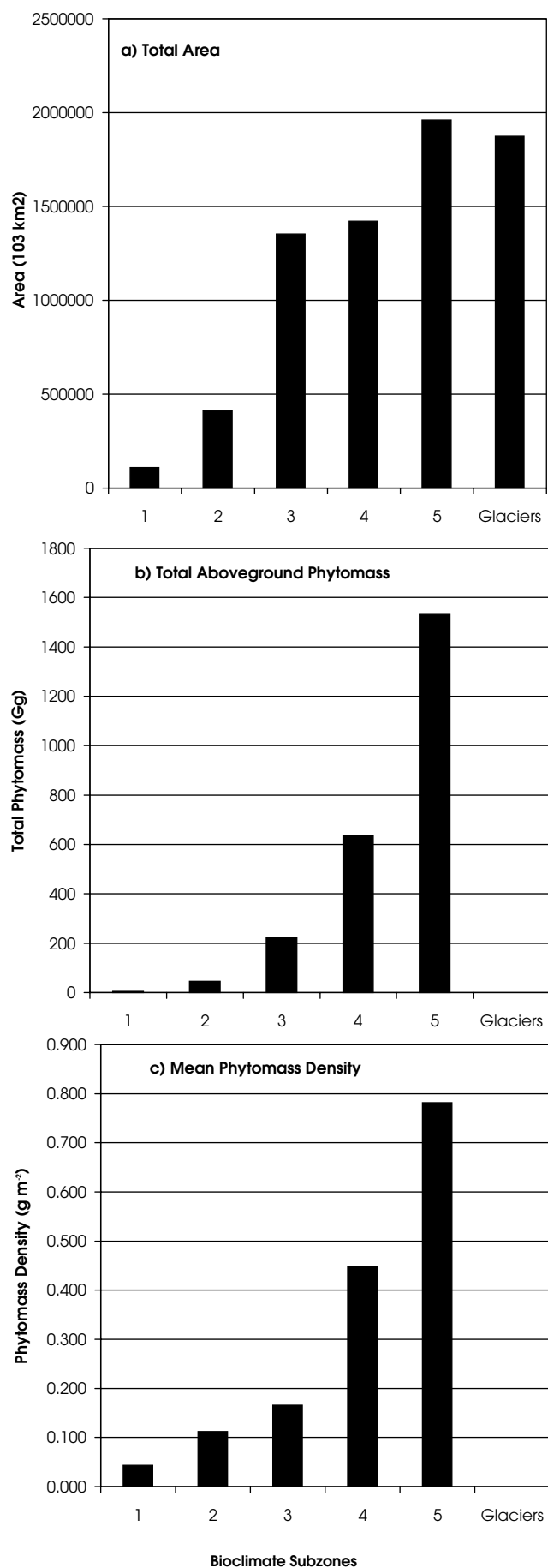
[38] The higher NDVI in MAT compared to MNT is consistent with earlier studies [Shippert *et al.*, 1995; Walker *et al.*, 1995, 1998]. Although MNT and MAT phytomass regression lines tend to diverge with warmer temperature (Figure 3a), the MSS-NDVI regression lines tend to converge (Figure 5b). This is probably caused by saturation of the MSS sensor at higher NDVI values [Shippert *et al.*, 1995; Tucker, 1976]. As vegetation density increases absorption approaches a maximum, beyond which additional vegetation density contributes minimally to the overall reflectance signature. The generally lower NDVI values of MNT were less subject to saturation than were the higher values of MAT. Previous studies have shown that saturation can occur in tundra vegetation with NDVI values between 0.6 and 0.8 [Shippert *et al.*, 1995]. This phenomenon is also seen with AVHRR data in the circumpolar extrapolation. The inclusion of the Council data in the regression (Figure 6) suggests saturation at NDVI at about 0.6 for this data set.

4.4. Circumpolar Extrapolation

[39] The Arctic bioclimate zone spans 30° of latitude, and the mean July temperature at sea level spans about $12^{\circ}C$. From treeline to the coldest areas of the Arctic, there is about a 30-fold difference in the maximum summer NDVI on zonal sites. This corresponds to more than a 100-fold difference in TAP on zonal sites (Figure 6). Other studies have noted about a tenfold difference in primary production [Bazilevich *et al.*, 1997], a fivefold difference in the number of vascular plants [Rannie, 1986], and a 50-fold difference in soil carbon [Bockheim *et al.*, 1996]. Our analysis provides the best available delineation of the area of the Arctic Zone and its subzones and the distribution of phytomass within the Arctic.

[40] Our estimate for the area of the Arctic is 7,115,000 km^2 , which is somewhat smaller than Bliss and Matveyeva's [1992] 7,567,000 km^2 . Our estimate of the total area within the High Arctic (subzones 1–3) is 1,600,000 km^2 compared to Bliss and Matveyeva's estimate of 198,400,000 km^2 . Our estimate for the Low Arctic (subzones 4 and 5) is 3,481,000 km^2 compared to 3,616,000 km^2 . Our estimate of ice cover is 2,034,000 km^2 compared to 1,967,000 km^2 . The area of the glaciers in the Arctic was greater than the landmass of any single subzone (Figure 7a).

[41] The map of the MaxNDVI (Figure 2a) gives a visual impression of the variation in phytomass across the Arctic.



There is, however, some uncertainty regarding biomass of NDVI values above about 0.55 because of the nonlinear relationship between NDVI and phytomass. Stratification of the circumpolar NDVI data according to subzones provides a means to examine transitions in phytomass across the bioclimatic gradient and insight into the nature of the subzones themselves. We found in both northern Alaska and the circumpolar region the expected shift to higher NDVI and phytomass toward the south. In northern Alaska, 90% of the estimated phytomass is concentrated in subzone 5. In the circumpolar analysis, 91% of the circumpolar phytomass is concentrated in the Low Arctic (subzones 4 and 5) (Figure 7b). The density of phytomass in subzone 5 is 16.8 times greater than the density within subzone 1 (47 versus 791 g m^{-2}) (Figure 7c). The High Arctic (subzones 1–3) covers about 22.5% of the Circumpolar Arctic, but has only about 9% of the total phytomass. The low phytomass in the High Arctic reflects the shorter, more open-growing vegetation and the relatively minor role that woody shrubs play in these colder northern subzones. Literature values for phytomass usually fall in the following ranges: polar desert (subzone 1), from 0 to 100 g m^{-2} ; polar semidesert (subzone 2), from 100 to 500 g m^{-2} ; typical arctic tundra (subzone 3) from 500 to 750; tussock tundra, 750 – 1000 g m^{-2} , and shrub tundra 2000 – 4000 g m^{-2} [Bliss and Matveyeva, 1992; Gilmanov, 1997; Shaver *et al.*, 1997]. Our estimates of phytomass density (g m^{-2}) for northern Alaska and the circumpolar Arctic were within the published ranges. There is a shift toward higher NDVI values from north to south through the subzones in all cases except the transition from subzone 2 to subzone 3, where there is a shift to lower NDVI and phytomass. One possible explanation of why the more northern subzone 2 has more biomass per unit area than subzone 3 was that subzone 3 has more mountains and high plateaus and may have a larger proportion in altitudinal zonal belts equivalent to subzones 2 and 1. Elevation was not considered in the analysis but it is an important source of variation to phytomass within the bioclimate subzones that should be considered in future analyses.

5. Conclusions

1. Total plant phytomass, LAI, and MaxNDVI increases with temperature along the climate gradient in northern Alaska. Our results support the general notion that there is a latitudinal greening in the Arctic associated with warmer temperatures.

2. The phytomass and NDVI are lower on nonacidic substrates than on acidic substrates. At the coast, total phytomass values on acidic and nonacidic sites are similar, but tend to diverge away from the coast with greater phytomass on acidic sites. The principal cause of the different response of MAT and MNT to temperature is the different species composition of the two types. The shrubs in MAT increase in height and biomass with greater summer

Figure 7. (opposite) Summary of information from the circumpolar analysis of the NDVI data in Figure 5a. (a) Area of the ice-free landmass of the five bioclimate subzones and glaciers within the Arctic. (b) Total phytomass (Gg). (c) Average phytomass density (g m^{-2}).

warmth; whereas, most shrub species in MNT are prostrate dwarf shrubs that show little change in stature with increased summer warmth. The phytomass of shrubs increased eightfold in MAT, but MNT shrub phytomass showed no correlation with temperature. Mosses show the greatest response to warming in MNT.

3. The phytomass of most PFTs increases with warmer temperatures except for sedges in nonacidic tundra and lichens in acidic tundra. Most of these responses are consistent with information from other studies; however, the strong increase in MNT moss phytomass has not been previously observed and needs to be confirmed with further studies.

4. The LICOR instrument offers a means to quickly obtain large quantities of LAI information for the vascular plant component of low Arctic vegetation, but it can not detect differences in LAI of the moss canopy, which proved to be important for this study. The instrument is also of limited use for extremely low-growing prostrate vegetation that is common on wind-blown sites and in the High Arctic.

5. This study provides considerable insight regarding the different response of dominant vegetation types and PFTs to climate change within the Low Arctic (subzones 4 and 5), and should be useful for developing dynamic global vegetation models. Our extrapolation of the phytomass values to the circumpolar Arctic provides a first approximation of total phytomass for the circumpolar region, but this is based on very few data at the end points of the climate gradient and a nonlinear regression that has considerable uncertainty at high NDVI values. More reliable estimates will require extending these types of studies into subzones 1–3 and the shrubbier portions of subzone 5. Future studies should also examine variation of biomass in wet and dry sites across the arctic climate gradient and at higher elevations.

[42] **Acknowledgments.** This study was funded by the NSF OPP-9908829 and an award from the International Arctic Research Center (IARC). We thank numerous students and research assistants who participated in this study including Monica Calef, Casey Dunn, Andrew Lillie, David Richardson, and David Wirth. Climate data were provided by several sources including Jim Ebersole, Larry Hinzman, Doug Kane, Walt Oechel, Tom Osterkamp, Vladimir Romanovsky, George Vourlitis, and the Toolik Lake LTER site.

References

- Bazilevich, N. I., A. A. Tishkov, and G. E. Vilchek, Live and dead reserves and primary production in polar desert, tundra and forest tundra of the former Soviet Union, in *Polar and Alpine Tundra*, pp. 509–539, Elsevier Sci., New York, 1997.
- Bliss, L. C., and N. V. Matveyeva, Circumpolar arctic vegetation, in *Arctic Ecosystems in a Changing Climate: An Ecophysiological Perspective*, pp. 59–89, Academic, San Diego, Calif., 1992.
- Bockheim, J. G., D. A. Walker, and L. R. Everett, Soil carbon distribution in nonacidic and acidic soils of Arctic Alaska, in *Advances of Soil Science, Proceedings of the International Symposium on Carbon Sequestration in Soil*, edited by R. Lal et al., pp. 143–155, CRC Press, Boca Raton, Fla., 1996.
- Carter, L. D., A Pleistocene sand sea on the Alaskan Arctic coastal plain, *Science*, *211*, 381–383, 1981.
- Chapin, F. S., III, and G. R. Shaver, Physiological and growth responses of arctic plants to a field experiment simulating climatic change, *Ecology*, *77*, 822–840, 1996.
- Chapin, F. S., III, S. A. Zimov, G. R. Shaver, and S. E. Hobbie, CO₂ fluctuation at high latitudes, *Nature*, *383*, 585–586, 1996.
- Clements, F. E., Nature and structure of the climax, *J. Ecol.*, *24*, 252–284, 1928.
- Edwards, E. J., A. Moody, and D. A. Walker, A western Alaskan transect to examine interactions of climate, substrate, vegetation, and spectral reflectance: ATLAS grids and transects, 1998–1999, unpublished data report, North. Ecosystem Anal. and Mapp. Lab., Univ. of Alaska Fairbanks, Fairbanks, AK, 2000.
- Elvebakk, A., Bioclimatic delimitation and subdivision of the Arctic, in *The Species Concept in the High North: A Panarctic Flora Initiative*, pp. 81–112, Norw. Acad. of Sci. and Lett., Oslo, 1999.
- Elvebakk, A., R. Elven, and V. Y. Razzhivin, Delimitation, zonal and sectorial subdivision of the Arctic for the Panarctic Flora Project, in *The Species Concept in the High North: A Panarctic Flora Initiative*, pp. 375–386, Norw. Acad. of Sci. and Lett., Oslo, 1999.
- Epstein, H. E., M. D. Walker, F. S. Chapin III, and A. M. Starfield, A transient, nutrient-based model of arctic plant community response to climate warming, *Ecol. Appl.*, *10*, 824–841, 2000.
- Gilmanov, T. G., Phenomenological models of the primary productivity of zonal arctic ecosystems, in *Global Change and Arctic Terrestrial Ecosystems, Ecol. Stud. Ser.*, vol. 124, pp. 402–436, Springer-Verlag, New York, 1997.
- Gilmanov, T. G., and W. C. Oechel, New estimates of organic matter reserves and net primary productivity of the North American tundra ecosystems, *J. Biogeogr.*, *22*, 723–741, 1995.
- Gough, L., G. R. Shaver, J. Carroll, D. L. Royer, and J. A. Laundre, Vascular plant species richness in Alaskan arctic tundra: The importance of soil pH, *J. Ecol.*, *88*, 54–66, 2000.
- Goward, S. N., B. Markham, and D. G. Dye, Normalized Difference Vegetation Index measurements from the Advanced Very High Resolution Radiometer, *Remote Sens. Environ.*, *35*, 257–277, 1991.
- Groisman, P. Y., T. R. Karl, and R. W. Knight, Observed impact of snow cover on the heat balance and the rise of continental spring temperatures, *Science*, *263*, 198–200, 1994.
- Hope, A. S., J. S. Kimball, and D. A. Stow, The relationship between tussock tundra, spectral reflectance properties, and biomass and vegetation composition, *Int. J. Remote Sens.*, *10*, 1861–1874, 1993.
- Jia, G. J., H. E. Epstein, and D. A. Walker, Spatial characteristics of AVHRR-NDVI along latitudinal transects in northern Alaska, *J. Veg. Sci.*, *13*, 315–326, 2002.
- Justice, C. O., J. R. G. Townshend, B. N. Holben, and C. J. Tucker, Analysis of the phenology of global vegetation using meteorological satellite data, *Int. J. Remote Sens.*, *6*, 1271–1318, 1985.
- Keeling, C. D., J. F. S. Chin, and T. P. Whorf, Increased activity of northern vegetation inferred from atmospheric CO₂ measurements, *Nature*, *382*, 146–149, 1996.
- Kittel, T. G. F., W. L. Steffen, and F. S. Chapin III, Global and regional modeling of Arctic-boreal vegetation distribution and its sensitivity to altered forcing, *Global Change Biol.*, *6*, 1–18, 2000.
- Markon, C. J., Characteristics of the Alaskan 1-km Advanced Very High Resolution Radiometer data sets used for analysis of vegetation biophysical properties, *USGS Open-File Rep. 99-088*, US Geol. Surv., Reston, Va., 1999.
- Markon, C. J., M. D. Fleming, and E. F. Binnian, Characteristics of vegetation phenology over the Alaskan landscape using AVHRR time-series data, *Polar Rec.*, *31*, 179–190, 1995.
- McMichael, C., A. S. Hope, D. A. Stow, J. B. Fleming, W. C. Oechel, and G. Vourlitis, Estimating CO₂ exchange in Arctic tundra ecosystems using a spectral vegetation index, *Int. J. Remote Sens.*, *20*, 683–698, 1999.
- Muller, S. V., A. E. Racoviteanu, and D. A. Walker, Landsat MSS-derived land-cover map of northern Alaska: Extrapolation methods and a comparison with photo-interpreted and AVHRR-derived maps, *Int. J. Remote Sens.*, *20*, 2921–2946, 1999.
- Myneni, R. B., C. D. Keeling, C. J. Tucker, G. Asrar, and R. R. Menani, Increased plant growth in the northern high latitudes from 1981 to 1991, *Nature*, *386*, 698–702, 1997.
- Oechel, W. C., G. Vourlitis, and S. J. Hastings, Cold-season CO₂ emission from arctic soils, *Glob. Biogeochem. Cycles*, *11*, 163–172, 1997.
- Rannie, W. F., Summer air temperature and number of vascular species in Arctic Canada, *Arctic*, *39*, 133–137, 1986.
- Shaver, F. R., A. E. Giblin, K. J. Nadelhoffer, and E. B. Rastetter, Plant functional types and ecosystem change in arctic tundras, in *Plant Functional Types*, pp. 153–173, Cambridge Univ. Press, New York, 1997.
- Shippert, M. M., D. A. Walker, N. A. Auerbach, and B. E. Lewis, Biomass and leaf-area index maps derived from SPOT images for Toolik Lake and Innavait Creek areas Alaska, *Polar Rec.*, *31*, 147–154, 1995.
- Smith, T., H. H. Shugart, and F. I. Woodward, *Plant Functional Types*, Cambridge Univ. Press, New York, 1996.
- Soil Survey Staff, *Keys to Soil Taxonomy*, 7th Edition, U.S. Dept. of Agric., Natl. Resour. Conserv. Serv., Washington, D. C., 1996.
- Steffen, W. L., B. H. Walker, J. S. I. Ingram, and G. W. Koch (Eds.), *Global Change and Terrestrial Ecosystem: The Operational Plan*, IGBP Rep. 21, Int. Biol. Programme, Stockholm, 1992.

- Stow, D., A. Hope, W. Boynton, S. Phinn, D. Walker, and N. Auerbach, Satellite-derived vegetation index and cover type maps for estimating carbon dioxide flux for Arctic tundra regions, *Geomorphology*, *21*, 313–327, 1998.
- Sturn, M., C. Racine, and K. Tape, Increasing shrub abundance in Arctic, *Nature*, *411*, 547–548, 2001.
- Tucker, C. J., Asymptotic nature of grass canopy spectral reflectance, *Appl. Opt.*, *16*, 1151–1156, 1976.
- Viovy, N., Arctic classification of time series (ACTS): A new clustering method for remote sensing time series, *Int. J. Remote Sens.*, *21*, 1537–1560, 2000.
- Vysotsky, G. N., Theses on soil and moisture (conspectus and terminology), in *Sbornik Lesnogo Observestva v Leningrad* (in Russian), pp. 67–79, Leningrad, Moskva, 1927.
- Walker, D. A., Height and growth rings of *Salix lanata* spp. *richardsonii* along the coastal temperature gradient in northern Alaska, *Can. J. Bot.*, *65*, 988–993, 1987.
- Walker, D. A., Hierarchical subdivision of arctic tundra based on vegetation response to climate, parent material, and topography, *Global Change Biol.*, *6*, 19–34, 2000.
- Walker, D. A., and K. R. Everett, Loess ecosystems of northern Alaska: Regional gradient and toposequence at Prudhoe Bay, *Ecol. Monogr.*, *61*, 437–464, 1991.
- Walker, D. A., and M. D. Walker, Terrain and vegetation of the Innavait Creek Watershed, in *Landscape Function: Implications for Ecosystem Disturbance, A Case Study in Arctic Tundra*, *Ecol. Stud. Ser.*, vol. 120, pp. 73–108, Springer-Verlag, New York, 1996.
- Walker, D. A., W. Acevedo, K. R. Everett, L. Gaydos, J. Brown, and P. J. Webber, Vegetation and a Landsat-derived land cover map of the Beechey Point Quadrangle, Arctic Coastal Plain, Alaska, *CRREL Rep. 87-5*, U.S. Army Cold Reg. Res. and Eng. Lab., Hanover, N. H., 1987.
- Walker, D. A., N. A. Auerbach, and M. M. Shippert, NDVI, biomass, and landscape evolution of glaciated terrain in northern Alaska, *Polar Rec.*, *31*, 169–178, 1995.
- Walker, D. A., et al., Energy and trace-gas fluxes across a soil pH boundary in the Arctic, *Nature*, *394*, 469–472, 1998.
- Walker, D. A., J. G. Bockheim, F. S. I. Chapin, W. Eugster, F. E. Nelson, and C. L. Ping, Calcium-rich tundra, wildlife, and the “Mammoth Steppe”, *Quat. Sci. Rev.*, *20*, 149–163, 2001.
- Walker, D. A., W. A. Gould, H. A. Maier, M. K. Reynolds, and S. V. Muller, The Circumpolar Arctic Vegetation Map: Environmental controls, AVHRR-derived base maps, and integrated mapping procedures, *Int. J. Remote Sens.*, *23*, 2552–2570, 2002.
- Westhoff, V., and E. van der Maarel, The Brown-Blanquet approach, in *Classification of Plant Communities*, edited by R. H. Whittaker, pp. 287–399, Kluwer Acad., Norwell, Mass., 1978.
- Williams, M., and E. B. Rastetter, Vegetation characteristics and primary productivity along an arctic transect: Implications for scaling-up, *J. Ecol.*, *87*, 885–898, 1999.
- Woodward, F. I., and W. Cramer, Plant functional types and climatic changes: Introduction, *J. Veg. Sci.*, *7*, 306–308, 1997.
- Young, S. B., The vascular flora of St. Lawrence Island with special reference to floristic zonation in the arctic regions, *Contrib. Gray Herb.*, *201*, 11–115, 1971.
- Yurtsev, B. A., Floristic division of the Arctic, *J. Veg. Sci.*, *5*, 765–776, 1994.

A. Balsler, C. Copass, E. J. Edwards, J. Hollingsworth, J. Knudson, H. A. Maier, A. Moody, M. K. Reynolds, and D. A. Walker, Institute of Arctic Biology, University of Alaska Fairbanks, Fairbanks, AK 99775-7000, USA. (ffdaw@uaf.edu)

H. E. Epstein and J. G. Jia, Department of Environmental Sciences, University of Virginia, Charlottesville, VA 22904-4123, USA.

W. A. Gould, International Institute of Tropical Forestry, USDA Forest Service, PO Box 25000, San Juan, Puerto Rico.

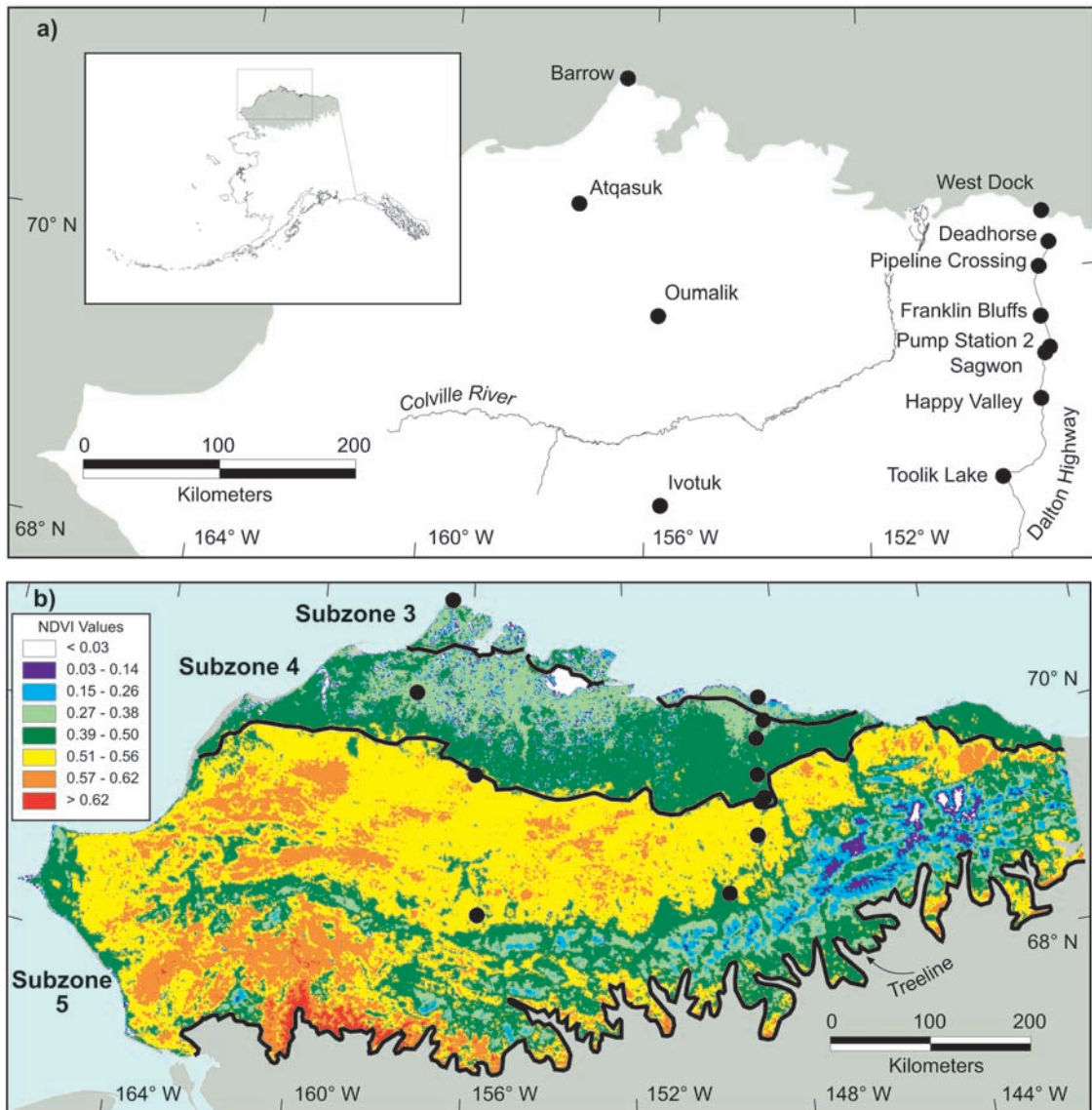


Figure 1. (a) Location of the field study sites on the Arctic Slope, Alaska, along an eastern transect, which follows the Dalton Highway, and a western transect in more remote areas. The inset map shows the tundra area north of treeline in gray. (b) MaxNDVI map of the area north of treeline with the locations of the study areas and the approximate boundaries of the bioclimate subzones.

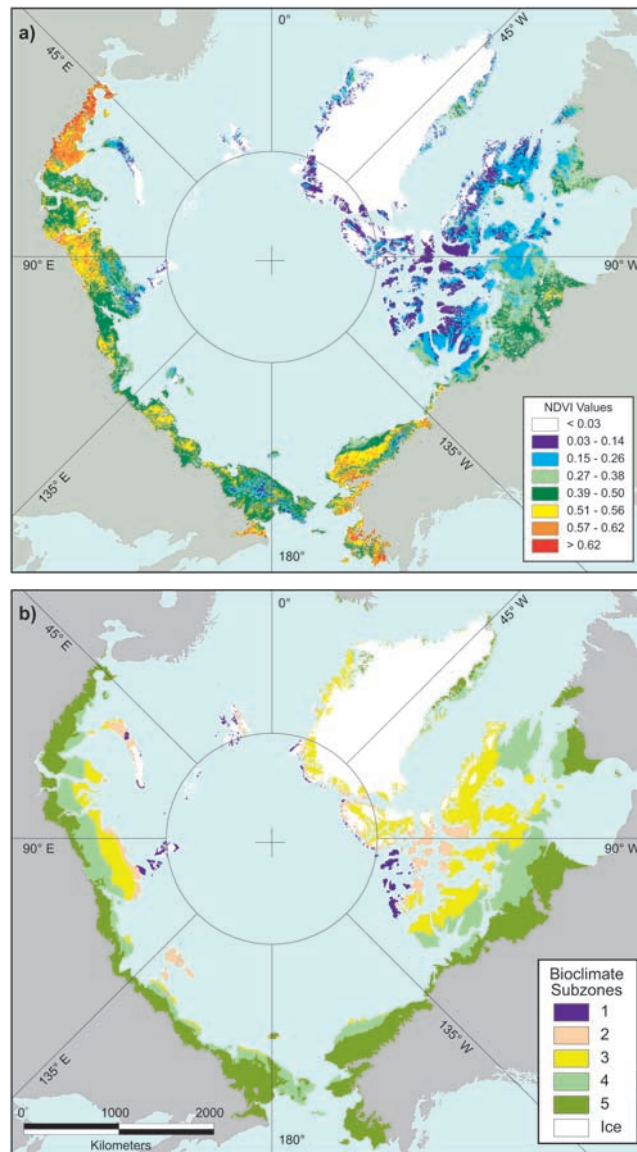


Figure 2. (a) Maximum NDVI of the Circumpolar Arctic. $NDVI = (NIR - R)/(NIR + R)$. NIR was the spectral reflectance in the near-infrared region of the spectrum ($0.725-1.1 \mu\text{m}$), where light scattering from the canopy dominates. R is the reflectance in the red chlorophyll-absorbing portion of the spectrum ($0.58-0.68 \mu\text{m}$). The image is derived from the pixels with the highest NDVI among biweekly images from 1993 and 1995 (relatively cloudless and snow-free years). The southern border of the CIR image is clipped to treeline, which was derived from the best available vegetation maps and expert knowledge. (b) Bioclimate subzones of the Arctic Tundra Zone. Subzones 1–5 are equivalent to subzones A–E of Walker *et al.* [2002]. The boundaries of the subzones were modified from the Arctic phytogeographic subzones of Yurtsev [1994] based on more recent information. Subzone 1 is the extreme polar desert subzone with mean July temperatures (MJT) less than 3°C and dominated by bare soil and scattered herbaceous plants, mosses, and lichens and no woody plants nor sedges. Subzone 2 is the prostrate dwarf-shrub subzone with MJT of $3-5^{\circ}\text{C}$. Subzone 3 is the hemiprostrate dwarf-shrub (*Cassiope*) subzone with MJT of $5-7^{\circ}\text{C}$. Subzone 4 is the erect dwarf-shrub subzone with MJT $7-9^{\circ}\text{C}$. Subzone 5 is the low-shrub (40–200 cm tall) subzone with MJT $10-12^{\circ}\text{C}$.

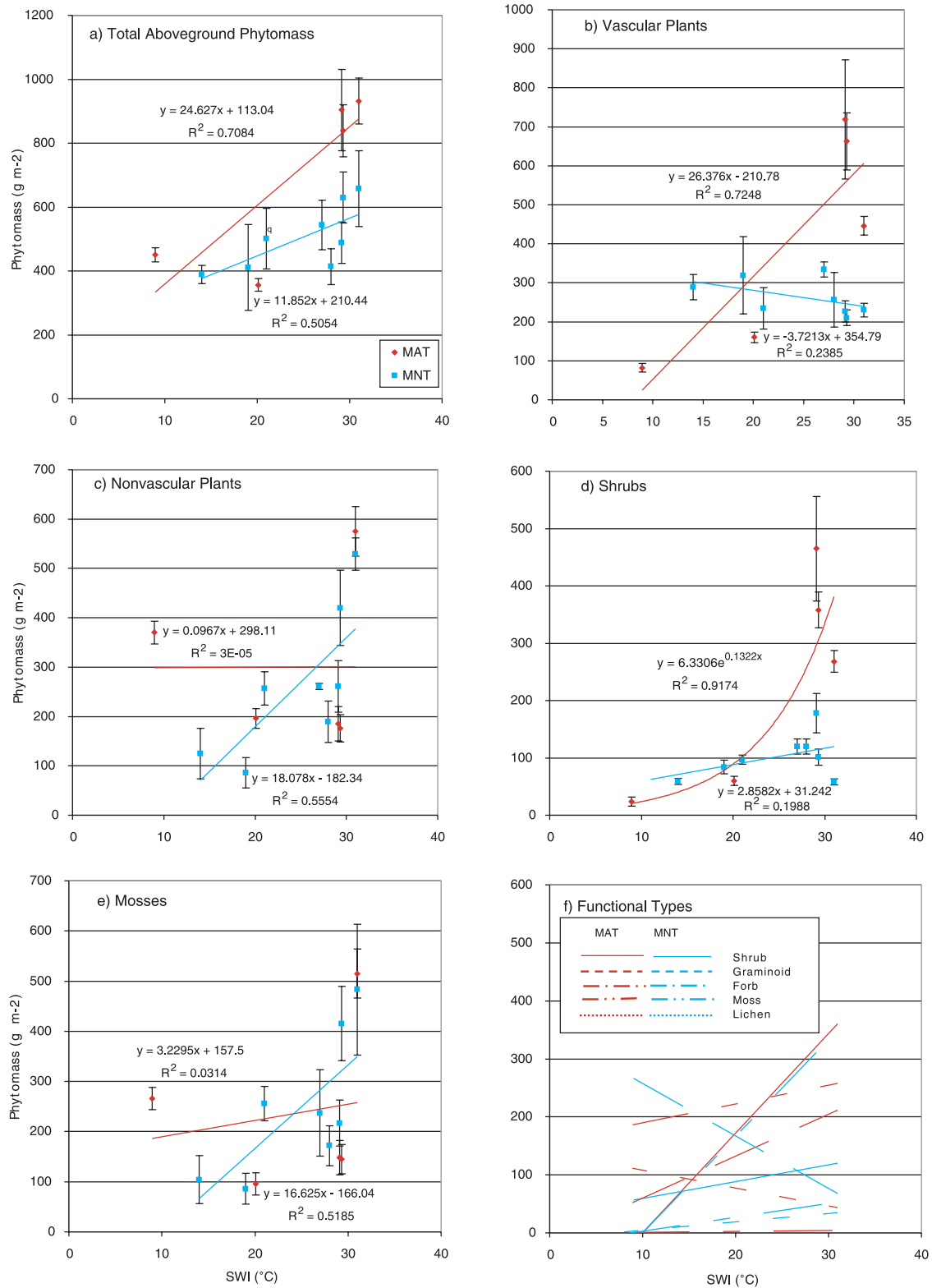


Figure 3. Phytomass (\pm standard error of the mean) along the summer warmth gradient: (a) TAP, (b) vascular plant phytomass, (c) nonvascular plant phytomass, (d) shrubs, (e) mosses, and (f) PFTs. The F statistic for all the regressions are significant at the 0.05 level, except the regressions for acidic nonvascular plants and mosses and nonacidic vascular plants.